



Research article

Investigation of key miRNAs and Target-mRNA in Kaposi's sarcoma using bioinformatic methods

Tianye Wang^{a,b,1}, Jun Zheng^{a,c,1}, Yangyang Pan^{a,c}, Zhaowei Zhuang^{a,c}, Yan Zeng^{a,c,*}

^a Precision Clinical Laboratory, Zhanjiang Central Hospital, Guangdong Medical University, Zhanjiang, Guangdong, China

^b Department of Epidemiology, School of Public Health, Fudan University, Shanghai, China

^c Key Laboratory of Xinjiang Endemic and Ethnic Disease, School of Medicine, Shihezi University, Shihezi, Xinjiang, China

A B S T R A C T

Kaposi's sarcoma (KS) is the second most common tumor in human immunodeficiency virus (HIV) infected patients worldwide. While many miRNAs have been confirmed to be involved in KS biological processes, no relevant studies have combined miRNA and mRNA expression profiles using KS patient tissue biopsies. In this study, we performed transcriptome sequencing on tumor and normal tissues from four KS patients and identified differentially expressed mRNA and miRNA, further performed target gene prediction and enrichment analysis. 19,551 target-mRNAs were identified by predicting 106 miRNAs, with 553 overlapping with 571 significantly differentially expressed mRNAs. Enrichment analysis showed significant involvement of the Ubiquitin-mediated proteolysis pathway. Additionally, the miRNA-mRNA interaction network was established, and the topological score of Cytoscape's algorithm was calculated for comparison with three other datasets. The Mutual Clustering Coefficient (MCC) scoring ranking placed ZBTB34, NFIB, and RORA as the top three mRNAs, while hsa-miR-16-5p, hsa-miR-27a-3p, hsa-miR-340-5p, hsa-miR-182-5p, and hsa-miR-186-5p ranked as the top five miRNAs. Hsa-miR-101-3p is the only miRNA that appears both in the top 10 MCC scores and at the intersection of the other two datasets. Finally, qRT-PCR was used to validate the findings at the cellular level. In summary, the miRNA analysis results indicated that hsa-miR-101-3p could be used as a potential diagnostic or therapeutic marker in future studies. Moreover, the mRNA analysis results suggested that the histone binding pathways involved in mRNAs and ubiquitin-related biological processes were closely associated with KS and could serve as promising biomarkers for the diagnosis and treatment of this disease.

1. Introduction

Kaposi's sarcoma (KS) is a malignancy originating from the endothelial lining of blood or lymphatic vessels, which leads to the formation of tumors or lesions, predominantly on the skin. These lesions may also impact the gastrointestinal tract, respiratory system, and oral cavity. The disease typically presents as red, purple, brown, or black spots on the skin. Classic KS predominantly affects elderly men of Mediterranean, Jewish, or Italian descent. However, KS is also common among HIV-positive individuals and is endemic in sub-Saharan Africa, where it affects both HIV-negative individuals and children. In these regions, KS can be a significant health concern; for instance, it was reported as the leading cause of cancer-related deaths in men in Mozambique and Uganda in 2020 [1]. First described by Moritz Kaposi in 1872 [2], the understanding of KS has continually evolved, revealing diverse epidemiological patterns and clinical manifestations.

MicroRNAs (miRNA) are short (~22 nucleotides), non-coding RNAs that regulate gene expression in all metazoan eukaryotes [3]. miRNAs are transcribed by RNA polymerase II to generate stem-loop hairpin structures, which are processed by Drosha and DGCR8 to

* Corresponding author. Key Laboratory of Xinjiang Endemic and Ethnic Disease, School of Medicine, Shihezi University, Shihezi, Xinjiang, China. E-mail address: zengyan910@gmail.com (Y. Zeng).

¹ Wang and Zheng contributed equally to this work.

produce precursor miRNAs. These precursor miRNAs are then further cleaved by Dicer and TRBP, leaving a 22-nt RNA duplex. One strand of the duplex is preferentially incorporated into RISC, which binds to complementary sequences in the 3' untranslated region (3' UTR) of target mRNAs, leading to translational inhibition or degradation [4]. Although each miRNA typically only modestly alters gene expression, individual miRNAs can have a broad impact by targeting hundreds of genes. Over 60 % of mammalian mRNAs contain conserved regions that serve as targets for miRNAs. In addition to the canonical pathway, non-canonical pathways for generating miRNAs also exist [5].

Accumulating evidence suggests that aberrant expression patterns of miRNAs are presented in many human malignancies, including KS. Highly expressed miRNAs may act as oncogenes by suppressing tumor suppressor genes, while miRNAs expressed at low levels may function as tumor suppressors by negatively regulating oncogenes [6]. Recent studies have described miRNA signatures in KS, with several miRNAs found to be downregulated or upregulated [7,8] as a mediator in the virus-host interaction network of KS [9]. These miRNAs have the potential to serve as biomarkers for KS diagnosis, prognosis prediction, and as targets for treatment.

It is frustrating that after over 150 years of discovering KS, the development mechanism of KS remains unclear. In recent years, RNA sequencing and bioinformatics analysis have enabled us to study molecular mechanisms in a new way and identify tumor-related genes. Regarding the differential expression of miRNA-mRNA target genes, Viollet et al. used KSHV-infected SLK cells in cell culture to reveal the interaction between miRNA and mRNA differential expression [10]. To date, there have been no relevant studies that have integrated miRNA and mRNA expression profiles using tissue biopsies from patients with Kaposi's sarcoma (KS). In this study, we conducted sequencing of both miRNA and mRNA from tumor and normal tissues of KS patients. The combined RNA sequencing data from these KS patient tissue biopsies are available for download on GEO (Gene Expression Omnibus) and PubMed. We further investigated the functions and pathways involved in these miRNA-mRNA interactions through cellular experiments to validate our findings. Our findings provide theoretical support for further studies of miRNA-mRNA interactions and cellular experiments with KSHV.

2. Material and methods

2.1. Data source

For sequencing analysis, we collected tumor and adjacent tissue samples from 4 patients with classic KS at Xinjiang Uyghur Autonomous Region Hospital, with confirmed pathological diagnoses between 2018 and 2021. All specimens were collected with informed consent from the study subjects or their families, numbered, and stored in liquid nitrogen after collection.

We also retrieved transcriptome sequencing data related to KS from the GEO database (<http://www.ncbi.nlm.nih.gov/geo>), including sequencing of miRNA or mRNA from both tumor and normal tissue biopsy samples of KS patients. We identified two datasets that met our criteria, of which GSE16353 [11] and GSE55625 [12] included miRNA sequencing results. In addition, we also searched PubMed and found a study by Muwonge et al. that sequenced miRNAs in the serum of KS patients and analyzed differentially expressed genes [13], which we included in our analysis.

2.2. Study procedure

Sequencing samples were prepared using both miRNA and mRNA libraries, followed by deep sequencing and subsequent bioinformatic analysis to identify differentially expressed genes and associated pathways. Results were merged with GEO and PubMed datasets for RRA analysis. Differential expressions of predicted mRNA and miRNA target genes were compared. Enrichment analysis was performed on the intersection of mRNA targets, which was then used to construct a miRNA-mRNA interaction network. The flow diagram of this study is shown in [Supplementary Fig. 1](#).

2.3. Bioinformatic analysis

We performed quality control on our raw data using FastQC and used Trimmomatic for the removal of low-quality bases and filtering of low-quality reads. Clean data was then aligned to the hg19 reference genome to determine gene expression levels. Differential gene analysis was performed using the limma package, and Gene Ontology (GO) analysis and Kyoto Encyclopedia of Genes and Genomes (KEGG) pathway enrichment analysis were conducted to identify differentially expressed genes. The miRNAs detected were compared by aligning Clean Data to the human mature miRNA sequences in the miRBase22 database. The Multimir tool was used to search for differentially expressed miRNA target genes in 14 validated databases, including miRecords, miRTarBase, and TarBase [14]. The output files were visualized using the UCSC Genome Browser (<http://www.genome.ucsc.edu>), and statistical analyses, heatmaps, and scatter plots were performed using the R suite software (<http://www.R-project.org>), employing the ggplot2 package for creating these visualizations.

2.4. Dataset preprocessing

The downloaded GEO datasets include matrix files for differential gene analysis using Deseq2. Muwonge et al.'s study directly extracted the top 50 differentially expressed genes. In this study, we obtained sequencing results and integrated them with the GEO datasets using RobustRankAggreg (RRA) to compare the ranking of differentially expressed genes from different sources [15]. The threshold points for differentially expressed genes (DEGs) were $\text{adj.P.Val} < 0.05$ and $|\log \text{fold change (FC)}| > 1$.

2.5. Construction of a miRNA-mRNA interaction network

Based on the analysis of differentially expressed miRNAs, differentially expressed mRNAs, and enriched pathways, a miRNA-mRNA regulatory network was visualized using Cytoscape [16]. Various topological algorithms (MCC, EPC) in cytohubba [17] were applied to calculate the scores of differentially expressed genes.

2.6. Cell culture

KSHV-infected cell lines (iSLK-219 and iSLK-BAC) and KSHV uninfected cell line (iSLK-Puro) were donated by Professor Ke Lan (Key Laboratory of Wuhan University) and cultured in DMEM high glucose medium (GIBCO, USA) containing 10 % fetal bovine serum, 100 $\mu\text{g}/\text{mL}$ G418, 4 $\mu\text{g}/\text{mL}$ puromycin, and 100 $\mu\text{g}/\text{mL}$ hygromycin (iSLK-Puro cells do not require hygromycin). KSHV positive B lymphoma cell lines (BC-3 and BCBL-1) and KSHV negative B lymphoma cell lines (BJAB), which were purchased from the American Type Culture Collection (ATCC), were cultured in RPMI1640 medium containing 10 % fetal bovine serum and 1 % antibiotics. All cells were cultured in an incubator containing 5 % CO_2 at 37 $^\circ\text{C}$.

2.7. RNA extraction and qRT-PCR

First, we extracted total RNA from cells using the Trizol method [18]; The RNA was then transcribed into cDNA using the Reverse Transcription Kit (RR047A, TaKaRa), and the cDNA was amplified using Universal Fluorescence Quantitative PCR Kit (BL697A, Biosharp). The qRT-PCR was performed under the following cycling parameters: 50 $^\circ\text{C}$ for 2 min, 95 $^\circ\text{C}$ for 10 min; 40 cycles at 95 $^\circ\text{C}$ for 15 s and 60 $^\circ\text{C}$ for 1 min; followed by melt-curve parameters: 95 $^\circ\text{C}$ for 15 s, 60 $^\circ\text{C}$ for 1 min, 95 $^\circ\text{C}$ for 15 s. The RNA transcript level was presented as relative quantification (RQ) using the comparative cycle threshold ($\Delta\Delta\text{CT}$) method. The relative expression was calculated based on the $2^{-\Delta\Delta\text{CT}}$ value, and all experiments were measured in triplicate. The miRNA levels were normalized against U6 levels. The primer sequences are detailed in [Supplementary Table 1](#).

3. Ethics statement

The study was approved by the Shihezi University (IIT-2017-004-01). Written informed consents were obtained from all study participants and the study did not interfere with the routine clinical care of the participants.

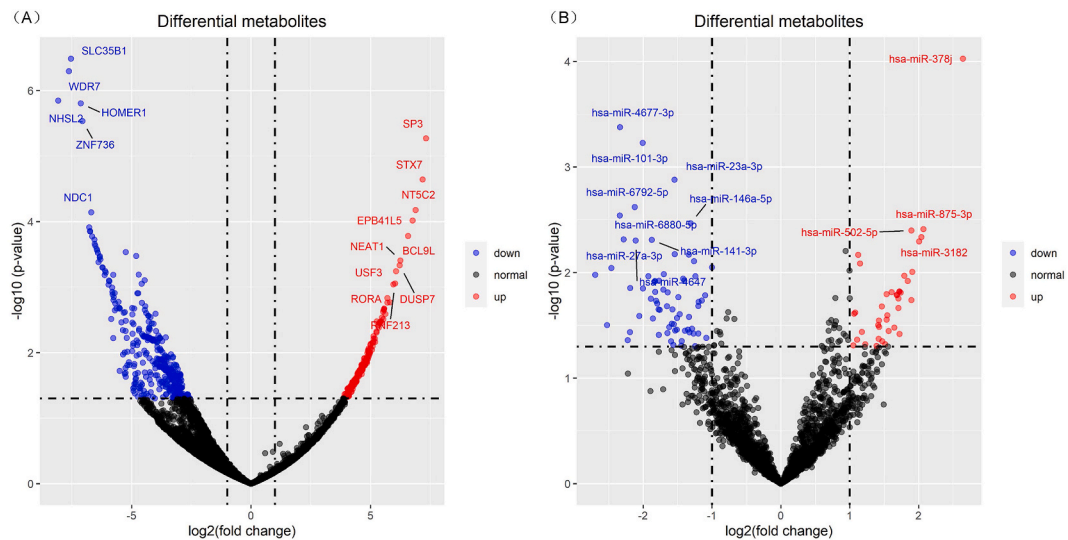


Fig. 1. The volcano plot for differential analysis of miRNA and mRNA. The limma package was applied to the sequencing results for differential analysis, and the volcano plot was drawn with a threshold of $|\log_{2}\text{FC}| > 1$, $p < 0.05$. **Fig. 1A** shows the differential analysis results for mRNA, with red indicating upregulated expression, blue indicating downregulated expression, and gray indicating no significant difference. 162 mRNAs were significantly upregulated, including SP3, STX7, NT5C2, EPB41L5, and NEAT1, which showed higher logFC values, suggesting more substantial upregulation. Among the 409 significantly downregulated mRNAs, SLC35B1, WDR7, HOMER1, NHSL2, and ZNF736 showed more significant downregulation. **Fig. 1B** shows the differential analysis results for miRNAs, with 39 miRNAs significantly upregulated and 67 miRNAs significantly downregulated.

4. Results

4.1. Differential analysis and enrichment analysis results

We compared the expression levels of miRNAs and mRNAs in KS tumor tissue and normal tissue. We found that in tumor tissue, 571 mRNAs and 106 miRNAs were significantly differentially expressed, with 162 upregulated and 409 downregulated mRNAs (Fig. 1A), 39 upregulated and 67 downregulated miRNAs (Fig. 1B). Notably, we observed more downregulated genes compared to upregulated ones.

Enrichment analysis showed that the GO analysis results were enriched in biological processes related to positive regulation of organelle organization, proteasome-mediated ubiquitin-dependent protein catabolic process, vacuolar membrane, lysosomal membrane, lytic vacuole membrane, and endoplasmic reticulum tubular network. The KEGG pathway analysis showed that the differentially expressed genes were enriched in pathways such as Ubiquitin mediated proteolysis, Protein processing in the endoplasmic reticulum, Circadian rhythm, mRNA surveillance pathway, and Autophagy – animal. Notably, both enrichment analysis results indicated that the differentially expressed genes were enriched in the Ubiquitin-mediated proteolysis pathway. This pathway ranked high, suggesting the importance of ubiquitin-mediated protein hydrolysis in the development of KS (Supplementary Table 2, Supplementary Table 3).

4.2. mRNA-miRNA interaction network

Using Multimir to search eight miRNA target gene databases and 106 significantly differentially expressed miRNAs, 19,551 target-mRNAs were identified. Comparison with 571 significantly differentially expressed mRNAs showed that 553 mRNAs were duplicated. The target genes of hsa-miR-16-5p, hsa-miR-27a-3p, and hsa-miR-340-5p had the largest intersection with the differentially expressed

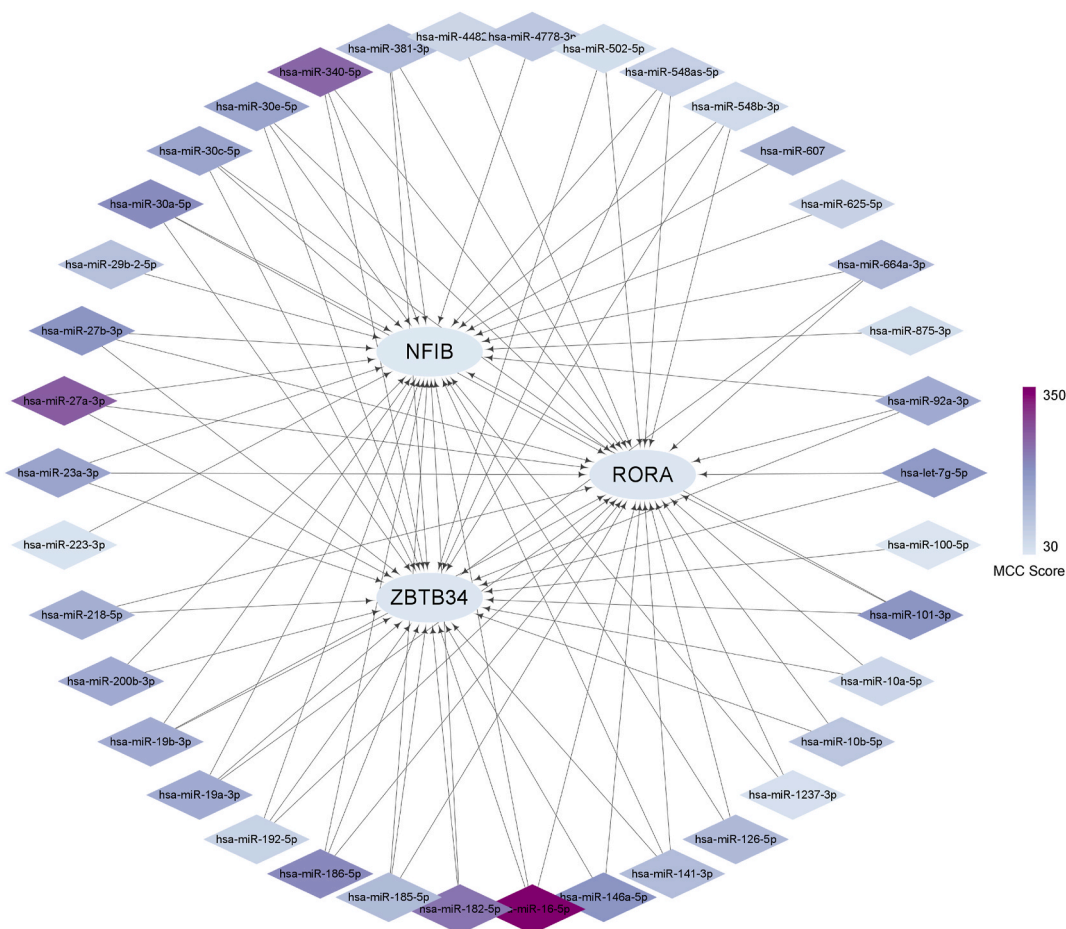


Fig. 2. The top 50 miRNA-mRNA networks with MCC scores. The miRNA-mRNA interaction network was constructed and scored based on the MCC score, and the darker the color, the higher the MCC score. Arrows indicate the targeted mRNA of miRNA. Only three mRNAs were identified among the top 50 miRNAs with high MCC scores, including ZBTB34, NFIB, and RORA.

mRNAs (Supplementary Table 4). A miRNA-mRNA interaction network was constructed, as shown in Supplementary Fig. 2, which contains 10 miRNAs, 50 predicted target genes and 310 interactions. These ten miRNAs potentially have a central role in the regulatory networks.

We used cytohubba-MCC score to rank the miRNA-mRNA interaction network [19], which is a centrality measure used for identifying the most densely interconnected clusters or cliques within a network. The top 50 genes with high scores are shown in Fig. 2, with ZBTB34, NFIB, and RORA ranking in the top three in mRNA, and hsa-miR-16-5p, hsa-miR-27a-3p, hsa-miR-340-5p, hsa-miR-182-5p, and hsa-miR-186-5p having MCC scores of over 200, consistent with the predicted target gene intersection results.

Table 1 shows the top ten miRNAs ranked by MCC score. In addition, using the RRA method to rank differentially expressed genes for the collected datasets, a Venn diagram (Fig. 3A) indicates that there were no genes differentially expressed in all four datasets, and three miRNAs were differentially expressed in three datasets. RRA results are shown in Fig. 3B, with a screening threshold set at $p < 0.05$ and $|\log_{2}FC| > 1$. The results showed that hsa-miR-625, hsa-miR-654, and hsa-miR-636 were significantly upregulated in two datasets, while hsa-miR-101, hsa-miR-1181, hsa-miR-185, and hsa-miR-1249 were significantly downregulated in two datasets. Of note, hsa-miR-101 was also ranked in the top ten by MCC score, indicating significant differential expression in KS tumor tissue.

Table 2 lists the top ten mRNAs ranked by MCC score. We selected the top 100 mRNAs ranked by MCC score (>18) for GO analysis, and the results are shown in Table 3. The analysis revealed significant enrichment in three pathways: endoplasmic reticulum tubular network, ATP-dependent chromatin remodeler activity, and histone binding. Compared with the enrichment analysis results of all genes, the differential genes were enriched in the endoplasmic reticulum tubular network pathway, indicating its essential role in the pathogenesis of KS. In addition, the differentially expressed genes TBL1XR1 and CBX5 in the histone binding pathway have high MCC scores in the interaction network, indicating that the histone binding pathway associated with TBL1XR1 and CBX5 could be key biomarkers for identifying KS.

4.3. qRT-PCR validation

Furthermore, we used qRT-PCR to verify validate whether these four miRNAs, including hsa-miR-101-3p (Fig. 4A), hsa-miR-186-5p (Fig. 4B), hsa-miR-27a-3p (Fig. 4C), and hsa-miR-27b-3p (Fig. 4D), were also significantly down-regulated at the cellular level. The results showed that the miRNAs expression in KSHV-infected cell lines iSLK-219 and iSLK-BAC and KSHV-positive B lymphoma cell lines BC-3 and BCBL-1 were significantly down-regulated compared with KSHV-uninfected cell lines iSLK-Puro and KSHV-negative B lymphoma cell line BJAB, which was consistent with the sequencing results.

5. Discussion

In the present study, we sequenced tumor and normal tissue samples from KS patients, analyzed mRNA and miRNA differential expression, and constructed an mRNA-miRNA interaction network. The results showed that the number of downregulated miRNAs was significantly higher than that of upregulated miRNAs (67 vs. 39), consistent with the conclusion of the three datasets included in this study [13,11,12]. Previous studies have shown that EBV-infected cells homologous to KSHV can activate miRNA expression suppressors, which is one of the reasons for downregulated miRNA expression [20]. Furthermore, KSHV encodes miRNAs to replace homologous miRNAs in infected cells, such as miR-K12-11 replacing hsa-miR-155, leading to downregulated miRNA expression [21].

We searched for mRNA sequencing data of KS tissue biopsies in the GEO database and PubMed. To date, Lidenge et al. is the only study that has conducted mRNA sequencing on KS tissue biopsies, with the dataset available as GSE147704. This study aimed to compare the expression profiles between endemic and epidemic KS. We downloaded the matrix file of this study from GEO and performed differential gene analysis using Deseq2. Among the 571 differentially expressed genes, 42 genes overlapped with those in our study, with the main pathways including proteasome-mediated ubiquitin-dependent protein catabolic process and ubiquitin ligase complex. These findings suggest that ubiquitin-related biosynthetic pathways may serve as potential biomarkers, which is consistent with the previous study on multi-ubiquitination regulation of p53 by LANA2 in KSHV [22].

Our study indicated that hsa-miR-101-3p was significantly downregulated in both datasets. Previous studies have shown that hsa-miR-101-3p was involved in various cancer processes, including colorectal cancer [23], renal cell carcinoma [24], prostate cancer [25], and bladder cancer [26], making it a potential biomarker for the diagnosis and prognosis. However, there is currently no research

Table 1
Top 10 miRNA in network ranked by MCC.

microRNA_id	MCC score	EPC score	logFC	P
hsa-miR-16-5p	344	97.473	-1.199	0.021
hsa-miR-27a-3p	257	91.959	-2.284	0.005
hsa-miR-340-5p	246	92.840	-1.773	0.039
hsa-miR-182-5p	231	89.968	-1.542	0.007
hsa-miR-186-5p	205	89.175	-2.463	0.009
hsa-miR-30a-5p	200	88.524	-1.338	0.007
hsa-miR-146a-5p	190	77.965	-1.310	0.003
hsa-miR-27b-3p	189	85.064	-1.769	0.012
hsa-miR-101-3p	188	84.264	-2.007	0.001
hsa-let-7g-5p	180	81.253	-1.243	0.011

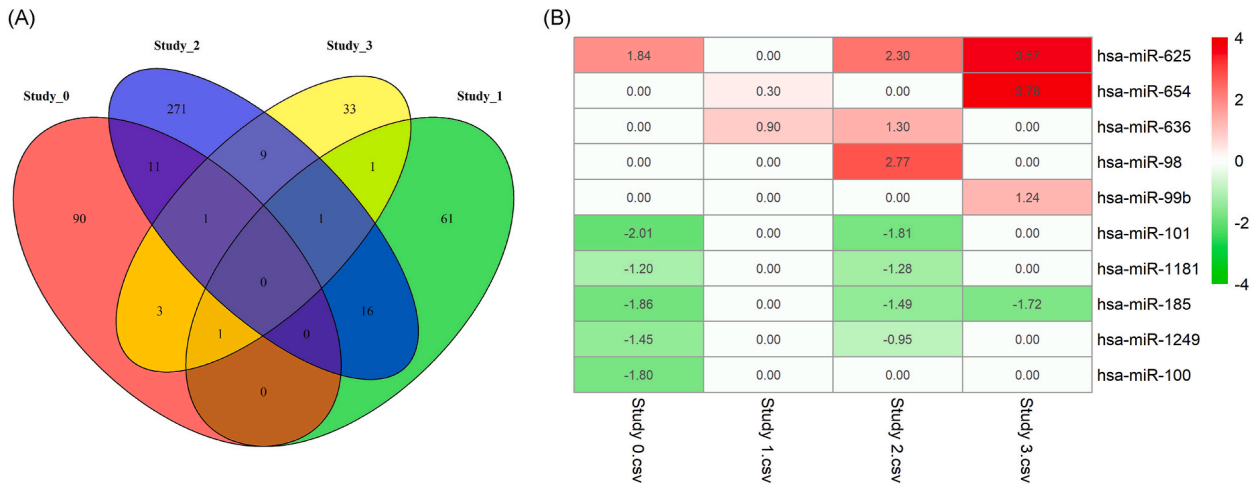


Fig. 3. Differential miRNA expression via RRA methods. Among the three datasets collected in this study (Studies 1–3) and our own sequencing results (Study 0). Fig. 3A shows the overlapping differential genes among the four datasets. Unfortunately, no miRNA was differentially expressed in all four datasets, but three miRNAs were significantly differentially expressed in three datasets. The RRA method was applied to calculate the differential expression of the four datasets, as shown in Fig. 3B. Red indicates upregulated miRNAs, green indicates downregulated miRNAs and blank values indicate no differential expression. Our results showed that hsa-miR-625, hsa-miR-654, and hsa-miR-636 were significantly upregulated in two or more datasets, while hsa-miR-101, hsa-miR-1181, hsa-miR-185, and hsa-miR-1249 were downregulated considerably in two or more datasets.

Table 2
Top 10 mRNA in network ranked by MCC.

mRNA_id	MCC score	EPC score	logFC	P
ZBTB34	37	52.345	-3.338	0.040
RORA	37	49.068	5.950	0.001
NFIB	34	49.591	-4.915	0.038
MAT2A	33	48.680	4.033	0.036
TBL1XR1	33	43.475	4.191	0.040
CBX5	33	50.483	4.593	0.017
HIPK2	33	52.678	4.056	0.047
SAMD8	32	45.736	-3.255	0.023
SRSF1	32	43.872	-4.246	0.026
RC3H1	31	45.277	4.896	0.009

Table 3
GO enrich result TOP 3.

Description	P	Gene_ID
endoplasmic reticulum tubular network	1.12×10^{-5}	ASPH/RAB10/ATL2/REEP3
ATP-dependent chromatin remodeler activity	1.68×10^{-5}	CHD1/CHD6/SMARCA5
histone binding	1.74×10^{-5}	TBL1XR1/CBX5/PHC3/RESF1/CHD1/CHD6/SMARCA5

linking miR-101 to KS. Based on existing research on miR-101, we speculate that the mechanism underlying its effect on KS development involves the downregulation of miR-101, which leads to an increase in the expression of PI3K and AKT genes, thereby promoting the activation of the PI3K/AKT pathway and inhibiting apoptosis [27]. In addition, the downregulation of miR-101 also promotes Wnt gene expression, activates the Wnt/beta-catenin pathway, and promotes cell proliferation and migration [28]. The significant downregulation of miR-101 observed in this study suggests that it could serve as a biomarker for the diagnosis and prognosis of KS.

We demonstrated the biological functions of differentially expressed mRNAs through GO and KEGG analysis and reviewed relevant literature. In ubiquitin-related biological processes, extensive research has shown the involvement of E3 ubiquitin ligase MDM2 with KS [29]. Additionally, the Kaposin B protein interacts with ubiquitin ligase, suppressing cell apoptosis [30]. Notably, the Kaposin protein also modulates the PI3K/Akt pathway [31], partially validating the conclusion of miR-101. There are ongoing studies related to the biological process of histone binding. For instance, the K-bZIP protein can bind to histones and alter the spatial structure of chromatin [32]. Additionally, KSHV infection results in various histone acetylation changes [33], which can affect DNA methylation

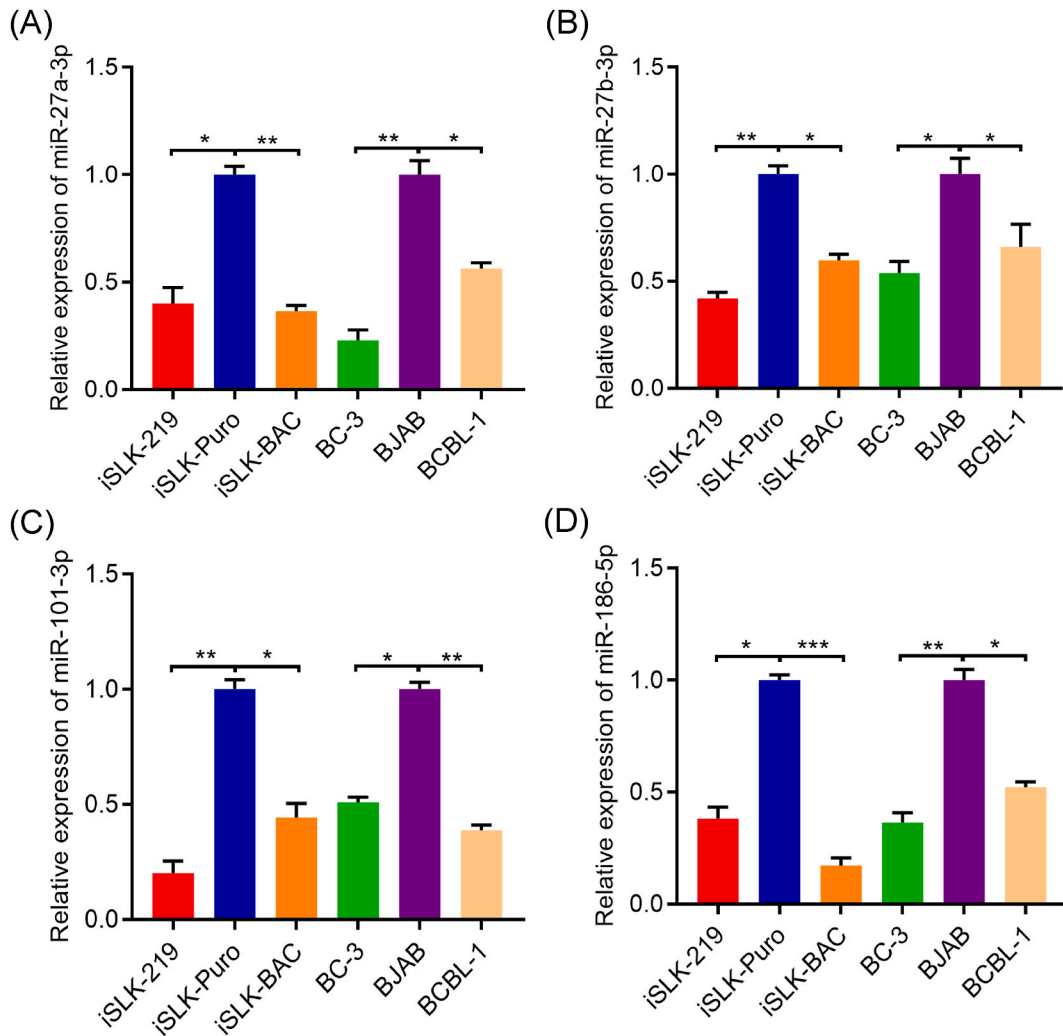


Fig. 4. Expression verification of related miRNAs via qRT-PCR. We performed qRT-PCR experiments to validate the results of data analysis by measuring the expression levels of four downregulated miRNAs, hsa-miR-27a-3p (Fig. 4A), hsa-miR-27b-3p (Fig. 4B), hsa-miR-101-3p (Fig. 4C), and hsa-miR-186-5p (Fig. 4D) in KSHV-positive and negative cell lines, iSLK-PURO and BJAB being KSHV-negative, and the other four cell lines being KSHV-positive. * denotes $p < 0.05$, ** denotes $p < 0.01$, and *** denotes $p < 0.001$. The results showed that compared to KSHV-positive cell lines, all four miRNAs were significantly downregulated in KSHV-negative cell lines, with statistical significance at the p-value level.

levels.

Various topological algorithms, including MCC, Degree, EPC, and BottleNeck, were used in cytohubba to calculate the scores of the differentially expressed genes. The experimental results showed that the MCC algorithm was stable [20]. In addition, the EPC scores are also given in Tables 1 and 2.

In addition, we performed qRT-PCR to validate the conclusions of data analysis at the cellular level. We chose hsa-miR-101-3p, hsa-miR-186-5p, hsa-miR-27a-3p, and hsa-miR-27b-3p for verification because, among the top ten miRNAs with MCC scores, miRNAs such as hsa-miR-16-5p have already been extensively studied and are closely related to the occurrence of various cancers [34]. In contrast, the miRNAs verified in this qRT-PCR have been less studied. Hsa-miR-27a and hsa-miR-27b, both of which are less studied in cancer-associated molecular mechanisms, are often combined in systematic reviews, suggesting their potential as biomarkers or molecular targets for tumors [35,36]; hsa-miR-101-3p, which has been found to be significantly downregulated in multiple KS datasets; hsa-miR-186-5p has the highest fold change value among differentially expressed miRNAs and lacks mechanistic research on its association with KS, were chosen for experimental validation. Our experimental results partially confirmed the accuracy of the data analysis.

As current research is mainly limited to cell experiments on KSHV infection. Therefore, our study significantly reveals potential molecular mechanisms and biomarkers for KS pathogenesis by sequencing KS patient tissues. However, our research has certain limitations. Firstly, we have not experimentally validated the accuracy and reliability of the target mRNA, which necessitates further experimental verification. Secondly, due to the limited availability of KS patients, our study included only four participants, leading

to substantial individual differences. Compared to Lidenge et al.'s study, which included 18 participants and screened out over 15,000 differentially expressed genes, future studies should expand the sample size of KS patients to obtain a complete miRNA-mRNA interaction network for KS patients.

In summary, by analyzing KS patient RNA-seq data, we identify the hub gene in the miRNA target gene network. Results of the analysis on miRNAs suggest that hsa-miR-101-3p can be used as a diagnostic and therapeutic marker in future studies. The results of mRNA analysis showed that the histone binding pathway involved in mRNAs such as TBL1XR1/CBX5 and ubiquitin-related biological processes were closely related to KS and could be used as biomarkers for the diagnostic and therapeutic procedures of KS.

Data availability statement

The data that support the findings of this study are available from the corresponding author upon reasonable request.

CRedit authorship contribution statement

Tianye Wang: Writing – original draft, Validation, Methodology, Formal analysis, Conceptualization. **Jun Zheng:** Validation, Methodology, Formal analysis. **Yangyang Pan:** Validation, Methodology, Formal analysis. **Zhaowei Zhuang:** Validation, Methodology, Formal analysis. **Yan Zeng:** Writing – review & editing, Writing – original draft, Supervision, Resources, Investigation, Funding acquisition, Formal analysis, Conceptualization.

Declaration of competing interest

The authors declare that they have no known competing financial interests or personal relationships that could have appeared to influence the work reported in this paper.

Acknowledgements

We would like to thank the patients for making this study possible. This study is supported by Natural Science Foundation of China (81772170), the Xinjiang Production and Construction Corps Science and Technology Cooperation Project (2021BC004); Zhanjiang High Level Hospital Construction Project (2021A05155); Central People's Hospital of Zhanjiang Startup Project of Doctor Scientific Research (2022A07); Shihezi University International Cooperation Project (GJHZ201901).

Appendix A. Supplementary data

Supplementary data to this article can be found online at <https://doi.org/10.1016/j.heliyon.2024.e29502>.

References

- [1] H. Sung, J. Ferlay, R.L. Siegel, et al., Global cancer statistics 2020: GLOBOCAN estimates of incidence and mortality worldwide for 36 cancers in 185 Countries, *CA A Cancer J. Clin.* 71 (3) (2021) 209–249.
- [2] G. Sternbach, J. Varon, Moritz Kaposi: idiopathic pigmented sarcoma of the skin, *J. Emerg. Med.* 13 (5) (1995) 671–674.
- [3] P. Bellare, D. Ganem, Regulation of KSHV lytic switch protein expression by a virus-encoded microRNA: an evolutionary adaptation that fine-tunes lytic reactivation, *Cell Host Microbe* 6 (6) (2009) 570–575.
- [4] T. Treiber, N. Treiber, G. Meister, Regulation of microRNA biogenesis and function, *Thromb Haemost* 107 (4) (2012) 605–610.
- [5] J. Yang, E.C. Lai, Alternative miRNA biogenesis pathways and the interpretation of core miRNA pathway mutants, *Mol. Cell* 43 (6) (2011) 892–903.
- [6] R. Visone, C.M. Croce, miRNAs and cancer, *Am. J. Pathol.* 174 (4) (2009) 1131–1138.
- [7] A.M. Catrina, I. Borze, M. Guled, et al., MicroRNA expression profiles in Kaposi's sarcoma, *Pathol. Oncol. Res.* 20 (1) (2014) 153–159.
- [8] S.B. Tuncer, B. Celik, D. Akdeniz Odemis, et al., miRNA sequence analysis in patients with Kaposi's sarcoma-associated herpesvirus, *Pathol. Oncol. Res.* (2022) 28.
- [9] D. Liang, X. Lin, K. Lan, Looking at Kaposi's sarcoma-associated herpesvirus–host interactions from a microRNA viewpoint, *Front. Microbiol.* 2 (2012).
- [10] C. Viollet, D.A. Davis, M. Reczko, et al., Next-generation sequencing analysis reveals differential expression profiles of miRNA-mRNA target pairs in KSHV-infected cells, *PLoS One* 10 (5) (2015) e126439.
- [11] A. Hansen, S. Henderson, D. Lagos, et al., KSHV-encoded miRNAs target MAF to induce endothelial cell reprogramming, *Genes Dev.* 24 (2) (2010) 195–205.
- [12] X.J. Wu, X.M. Pu, Z.F. Zhao, et al., The expression profiles of microRNAs in Kaposi's sarcoma, *Tumour Biol* 36 (1) (2015) 437–446.
- [13] H. Muwonge, H. Kasujja, N. Niyonzima, et al., Unique circulating microRNA profiles in epidemic Kaposi's sarcoma, *Non-coding RNA Research* 7 (2) (2022) 114–122.
- [14] Y. Ru, K.J. Kechris, B. Tabakoff, et al., The multiMiR R package and database: integration of microRNA–target interactions along with their disease and drug associations, *Nucleic Acids Res.* 42 (17) (2014) e133.
- [15] R. Kolde, S. Laur, P. Adler, et al., Robust rank aggregation for gene list integration and meta-analysis, *Bioinformatics* 28 (4) (2012) 573–580.
- [16] P. Shannon, A. Markiel, O. Ozier, et al., Cytoscape: a software environment for integrated models of biomolecular interaction networks, *Genome Res.* 13 (11) (2003) 2498–2504, <https://doi.org/10.1101/gr.1239303>.
- [17] C.H. Chin, S.H. Chen, H.H. Wu, C.W. Ho, M.T. Ko, C.Y. Lin, cytoHubba: identifying hub objects and sub-networks from complex interactome, *BMC Syst. Biol.* 8 (Suppl 4) (2014) S11, <https://doi.org/10.1186/1752-0509-8-S4-S11>. Suppl 4.
- [18] Endrit Elbasani, et al., Kaposi's sarcoma-associated herpesvirus lytic replication is independent of anaphase-promoting complex activity, *J. Virol.* 94 (13) (2020) e02079, <https://doi.org/10.1128/JVI.02079-19>, 19.

- [19] H. Ma, Z. He, J. Chen, et al., Identifying of biomarkers associated with gastric cancer based on 11 topological analysis methods of CytoHubba, *Sci. Rep.* 11 (1) (2021).
- [20] S.E. Godshalk, S. Bhaduri-Mcintosh, F.J. Slack, Epstein-Barr virus-mediated dysregulation of human microRNA expression, *Cell Cycle* 7 (22) (2008) 3595–3600.
- [21] E. Gottwein, N. Mukherjee, C. Sachse, et al., A viral microRNA functions as an orthologue of cellular miR-155, *Nature* 450 (7172) (2007) 1096–1099.
- [22] M. Laura, C.F.D.L. Cruz-Herrera, A. Ferreirós, et al., KSHV latent protein LANA2 inhibits sumo2 modification of p53, *Cell Cycle* 14 (2) (2015) 277–282.
- [23] L. Tao, C. Xu, W. Shen, et al., HIPK3 inhibition by exosomal hsa-miR-101-3p is related to metabolic reprogramming in colorectal cancer, *Front. Oncol.* 11 (2022).
- [24] X. Xu, C. Liu, J. Bao, Hypoxia-induced hsa-miR-101 promotes glycolysis by targeting TIGAR mRNA in clear cell renal cell carcinoma, *Mol. Med. Rep.* 15 (3) (2017) 1373–1378.
- [25] R.B. Duca, C. Massillo, G.N. Dalton, et al., MiR-19b-3p and miR-101-3p as potential biomarkers for prostate cancer diagnosis and prognosis, *Am. J. Cancer Res.* 11 (6) (2021) 2802–2820.
- [26] X. Rao, H. Cao, Q. Yu, et al., NEAT1/MALAT1/XIST/PKD-Hsa-Mir-101-3p-DLGAP5 Axis as a novel diagnostic and prognostic biomarker associated with immune cell infiltration in bladder cancer, *Front. Genet.* 13 (2022).
- [27] Y. Lei, Q. Wang, L. Shen, et al., MicroRNA-101 suppresses liver fibrosis by downregulating PI3K/Akt/mTOR signaling pathway, *Clinics and Research in Hepatology and Gastroenterology* 43 (5) (2019) 575–584.
- [28] H. Wang, Y. Meng, Q. Cui, et al., MiR-101 targets the EZH2/Wnt/ β -catenin the pathway to promote the osteogenic differentiation of human bone marrow-derived mesenchymal stem cells, *Sci. Rep.* 6 (1) (2016).
- [29] S. Varmazyar, S.M. Marashi, Z. Shoja, et al., MDM2 gene polymorphisms and risk of classic Kaposi's sarcoma among Iranian patients, *Med. Microbiol. Immunol.* 206 (2) (2017) 157–163.
- [30] M. Kleer, G. Macneil, N. Adam, et al., A panel of Kaposi's sarcoma-associated herpesvirus mutants in the polycistronic Kaposin locus for precise analysis of individual protein products, *J. Virol.* 96 (5) (2022) e156021.
- [31] F. Zhou, M. Xue, D. Qin, et al., HIV-1 Tat promotes Kaposi's sarcoma-associated herpesvirus (KSHV) vIL-6-induced angiogenesis and tumorigenesis by regulating PI3K/PTEN/AKT/GSK-3 β signaling pathway, *PLoS One* 8 (1) (2013) e53145.
- [32] F.P. Martínez, Q. Tang, Leucine zipper domain is required for Kaposi sarcoma-associated herpesvirus (KSHV) K-bZIP protein to interact with histone deacetylase and is important for KSHV replication, *J. Biol. Chem.* 287 (19) (2012) 15622–15634.
- [33] R.K. Singh, D. Bose, E.S. Robertson, Epigenetic reprogramming of Kaposi's sarcoma-associated herpesvirus during hypoxic reactivation, *Cancers* 14 (21) (2022) 5396.
- [34] S. Ghafouri-Fard, T. Khoshbakht, B.M. Hussien, et al., A review on the role of mir-16-5p in the carcinogenesis, *Cancer Cell Int.* 22 (1) (2022).
- [35] D. Qatrun Nada, M.L. Masniza, N. Abdullah, et al., Distinct microRNA expression pattern in breast cancer cells following anti-neoplastic treatment: a systematic review and functional analysis of microRNA target genes, *Malays. J. Pathol.* 44 (3) (2022) 367–385.
- [36] T.A.B.D. Santana, L. de Oliveira Passamai, F.S. de Miranda, et al., The role of miRNAs in the prognosis of triple-negative breast cancer: a systematic review and meta-analysis, *Diagnostics* 13 (1) (2023) 127.